



**HAL**  
open science

# Bayesian Identification of Surrogate Microstructure Generators

Philipp Eisenhardt, Ustim Khristenko, Barbara Wohlmuth, Andrei Constantinescu

► **To cite this version:**

Philipp Eisenhardt, Ustim Khristenko, Barbara Wohlmuth, Andrei Constantinescu. Bayesian Identification of Surrogate Microstructure Generators. 16ème Colloque National en Calcul de Structures (CSMA 2024), CNRS; CSMA; ENS Paris-Saclay; CentraleSupélec, May 2024, Hyères, France. hal-04610900

**HAL Id: hal-04610900**

**<https://hal.science/hal-04610900v1>**

Submitted on 3 Dec 2024

**HAL** is a multi-disciplinary open access archive for the deposit and dissemination of scientific research documents, whether they are published or not. The documents may come from teaching and research institutions in France or abroad, or from public or private research centers.

L'archive ouverte pluridisciplinaire **HAL**, est destinée au dépôt et à la diffusion de documents scientifiques de niveau recherche, publiés ou non, émanant des établissements d'enseignement et de recherche français ou étrangers, des laboratoires publics ou privés.

# Bayesian Identification of Surrogate Microstructure Generators

P. Eisenhardt<sup>1</sup>, U. Khristenko<sup>2</sup>, B. Wohlmuth<sup>3</sup>, A. Constantinescu<sup>1</sup>

<sup>1</sup> LMS, Ecole Polytechnique, {philipp.eisenhardt, andrei.constantinescu}@polytechnique.edu

<sup>2</sup> Digital Sciences & Technologies Department, Safran Tech, ustim.khristenko@safrangroup.com

<sup>3</sup> Department of Mathematics, Technical University of Munich, wohlmuth@ma.tum.de

**Abstract** — The generation of heterogeneous microstructures using surrogate models plays an important role in order to quantify the resultant material properties given only limited specimen. Using Gaussian Random Fields, material microstructure realizations can be obtained through a surrogate model from which new realizations can quickly be generated. The given paper explores the opportunities of identifying the surrogate model parameters using Bayesian Inference. The use of stochastic methods enables the future application to uncertainty propagation, for example in the area of reliability analysis.

**Mots clés** — Inverse Problems, Microstructure Identification, Surrogate Materials Models.

## 1 Introduction

The microstructure of a given specimen plays a large role in defining its effective material properties, making material microstructure characterization a central problem in engineering science. It has effects on local physical fields, computational homogenization and failure prediction (see [2, 10] and the references therein).

Without loss of generality of the present approach for various physical field equations, this is shown as an example for linear elasticity. For a domain  $\mathcal{D}$  written with and without periodic boundary condition, this leads to the linear elastic boundary value problem

$$\begin{cases} \operatorname{div} \mathbb{C}(\mathbf{x}) : \boldsymbol{\varepsilon} = \mathbf{0} & \text{in } \mathcal{D} \\ \boldsymbol{\varepsilon} = \nabla^s \mathbf{u} & \text{in } \mathcal{D} \\ \mathbf{u}(\mathbf{x}) = \hat{\mathbf{u}} & \text{on } \partial\mathcal{D}_d \\ \mathbb{C}(\mathbf{x}) : \boldsymbol{\varepsilon} \cdot \mathbf{n} = \hat{\mathbf{t}} & \text{on } \partial\mathcal{D}_t \end{cases} \quad (1)$$

with

$\mathcal{D} \in \mathbb{R}^n$ : Computational Domain,	$\mathbb{C}$ : Locally Dependent Elasticity Tensor,
$\mathbf{x} \in \mathbb{R}^n$ : Spatial Coordinate,	$\boldsymbol{\varepsilon}$ : Strain and Symmetric Gradient of Displacement,
$\partial\mathcal{D}_d$ : Dirichlet Boundary part of $\mathcal{D}$ ,	$\hat{\mathbf{u}}$ : Predefined Boundary Displacement,
$\partial\mathcal{D}_t$ : Neumann Boundary part of $\mathcal{D}$ ,	$\hat{\mathbf{t}}$ : Predefined Boundary Stress.

From the problem of linear elasticity the need for a spatial representation of the material microstructure, here shown for  $\mathbb{C}$ , can be seen as this will affect the resulting field variable  $\mathbf{u}$ . The microstructure is governed by the local variations in mechanical properties, which holds true for other field problems.

For numerical methods its representation is required. Using material specimens this can, depending on the type of specimen, be gathered using Electron Backscatter Diffraction (EBSD) or  $\mu$ CT measurements. An overview of practical identification methods can be found in [3]. This leads to measurements as the one shown in figure 1, adapted from [6, 7], where a porous pyrocarbon matrix is displayed. The assignment of the elastic parameters as needed for equation 1 would be conducted based on material measurements, indicated by the colour at the respective positions.

The obtained microstructure can then be characterized by different descriptors. One of the most common is the Two Point Correlation Function  $S_2$  which for binary microstructures measures the correlation between two points, see [10] for other descriptors and their interpretation. This characterization can be used to assess the similarity between different microstructures.

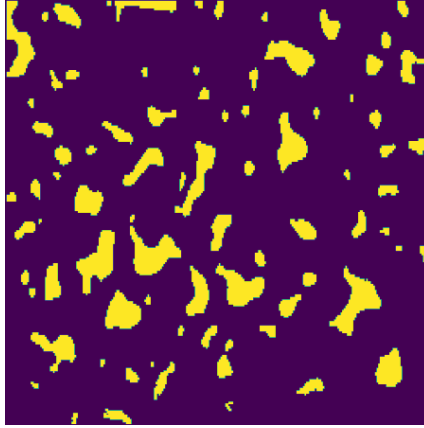


Figure 1: Example Microstructure of porous pyrocarbon from nuclear buffer structure, adapted from [7] under CC-BY 4.0

Surrogate microstructure samples can be used to complement the limited real microstructure data to conduct statistical analysis of the effective material properties and the structural response. Here, a functional representation of the material microstructure is sought from which new samples can be easily computed. An overview of different surrogate microstructure generators can be found in [2].

In the given paper, the identification of surrogate microstructure generators based on a *Random Field Approach* is studied. Here, the microstructure morphology is parameterized through tunable parameters which are determined using *Bayesian Inference* comparing surrogate samples to ground truth microstructures. The use of Bayesian inference enables further studies based on uncertainty propagation of the posterior likelihood from the resulting parameters. Here, the microstructures are generated through a *Gaussian Random Field* as in [9] and compared to ground truth microstructures using the  $S_2$  correlation function described in [10].

The report is structured in three parts. The approach is described in 2. The results of the identification based on an artificially generated microstructure sample are presented in 3. Some potential future extensions are introduced in 4.

## 2 Numerical Procedure

In order to find a description of a microstructure's elasticity parameters suitable for field problems as presented in equation 1, the microstructure's material type at different points needs to be related to the local elasticity parameters. Given a parametric description  $\chi$  of a microstructure for the binary case, this can be expressed as

$$\mathbb{C}(\mathbf{x}) = \chi(\mathbf{x}, \boldsymbol{\theta}, \boldsymbol{\omega})\mathbb{C}_1 + (1 - \chi(\mathbf{x}, \boldsymbol{\theta}, \boldsymbol{\omega}))\mathbb{C}_2.$$

Here, the microstructure depends on  $\boldsymbol{\theta}, \boldsymbol{\omega}$ , where  $\boldsymbol{\theta} \in \mathbb{R}^d$  are the tunable parameters and  $\boldsymbol{\omega} \in \Omega$  is the sample indicator. From  $\chi$ , different realizations can be sampled in turn giving rise to different overall elastic behaviours affecting the resulting effective material properties.

For the inverse problem, the tunable parameters  $\boldsymbol{\theta}$  are treated as random variables to be inferred through *Bayesian Inferences* and Markov Chain Monte Carlo. The identification is based on the knowledge of material microstructure samples  $\chi^{\text{data}}$ , such that realizations from  $\chi^{\text{model}}$  closely capture the morphological properties of the ground truth.

Once a description of  $\boldsymbol{\theta}$  has been obtained, new microstructure samples can be generated.

### 2.1 Surrogate Microstructure Generation

In this report, the surrogate samples are generated using a Gaussian Random Field based approach. This means, the level set describing the microstructure is generated based upon a Gaussian Random Field as laid out in [8]. For the moment, the problem is restricted to the binary microstructure problem, though

an extension to further constituents is possible <sup>1</sup>. Once the surrogate function has been identified, further realizations of samples can be generated.

**Level Set Cutoff** The material microstructure is derived from a random field  $q$  by conducting a level set cut of said field. As shown in [8], this process can be written as

$$\chi(\mathbf{x}, \omega) = \begin{cases} 1, & \text{if } q(\mathbf{x}, \omega) \geq \tau, \text{inclusion} \\ 0, & \text{if } q(\mathbf{x}, \omega) < \tau, \text{matrix.} \end{cases} \quad (2)$$

This leads to the level set parameter  $\tau$ , which can be related to the volume fraction of each component. Using the indicator function  $\chi(\mathbf{x}, \omega)$ , further material properties as local elasticity tensors or other properties can be assigned.

**Random Field Generation** The level set  $q(\mathbf{x}, \theta, \omega)$ , which depends on the spatial location  $\mathbf{x} \in \mathcal{D}$ , tunable parameters  $\theta \in \mathbb{R}^d$  and the sample indicator  $\omega \in \Omega$  is sampled through a Gaussian Random Field. To generate a realization of the Gaussian Random Field a homogeneous covariance function is introduced. This means, the covariance between two points only depends on their distance. Here, the covariance is chosen to be of Matérn type, which is a widely adopted hypothesis. This leads to

$$C(\mathbf{x}, \mathbf{y}) = \mathcal{M}_\nu \left( \frac{\sqrt{2\nu}}{l} \|\mathbf{x} - \mathbf{y}\|_A \right) \quad \mathcal{M}_\nu(\mathbf{x}) = \frac{\mathbf{x}^\nu \mathcal{K}_\nu(\mathbf{x})}{2^{\nu-1} \Gamma(\nu)}, \quad (3)$$

giving  $\mathcal{M}_\nu$  as the normalized Matérn kernel, where  $\mathcal{K}_\nu$  is the modified Bessel function of second kind and  $\Gamma$  is the gamma function;  $\nu$  is a smoothness parameter defining how many times the resulting random field will be differentiable. To sample a random field with a covariance in the form of equation 3, Gaussian white noise can be correlated by computing the convolution of the covariance kernel with white noise using the Fast Fourier Transformation (FFT).

**Tunable Paramters** In the presented model the tunable parameters consist of volume fraction, correlation length, smoothness and anisotropy. They were combined into a set  $\theta$  with

$$\theta = \{\tau, l, \nu, \mathbf{A}\},$$

however, in the presented approach, the resulting random field was assumed to be twice differentiable as a cutoff is conducted. Additionally, the microstructure is assumed to be isotropic, thus implying  $\mathbf{A} = \mathbf{I}$ . This leads to

$$\theta = \{\tau, l\}. \quad (4)$$

**Generation Code** The previous steps can be shown in algorithm 1. Using this approach for different parameters  $\theta$ , the effect the parameters have on resulting microstructures are illustrated in figure 2.

---

**Algorithm 1:** Morphology Based Metamodel

---

**Data:** Surrogate Parameters  $\theta = \{\tau, l\}$

**Result:** Realization of Surrogate Microstructure

```

/* Algorithm to generate surrogate samples given the model parameters */
def generateSampleMorphology(l: float, tau: float):
    /* Generate binary microstructure with Matérn Covariance function and given correlation
       length and volume fraction */
    Generate Matérn Covariance;
    Sample Gaussian Noise  $\eta$ ;
     $q \leftarrow$  Through Convolution of Matérn Kernel with  $\eta$  using FFT// Covariance from 3
     $\chi \leftarrow$  Level set cut from  $q$ // Cut according to 2
    return  $\chi$ ;

```

---

<sup>1</sup>The process for this laid out in Section 5.2 in [9] includes multiple level sets with the section assignment being done with the dominant one at each pixel/ voxel.

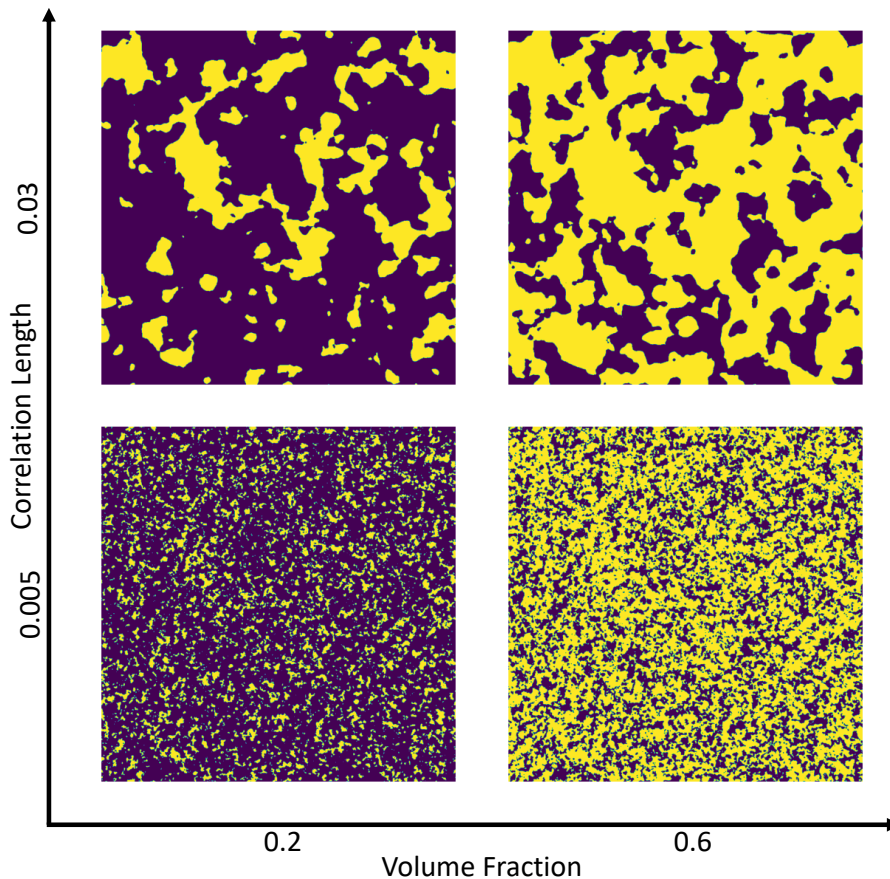


Figure 2: Comparison of sample Morphologies by the phase indicator function  $\chi(\mathbf{x})$  with their covariance and level set parameters (volume fraction and correlation length), phases indicated by colour

## 2.2 Identification Surrogate Model Parameters

To generate surrogate microstructures similar to measured samples, the parameters  $\theta$  of the surrogate model need to be tuned. Once the tuned parameter set has been obtained, realizations of the surrogate material can be generated using algorithm 1.

The covariance kernel properties are obtained from a numerically generated *ground truth* sample as an artificial toy problem to validate the approach. This inverse problem is solved by Bayesian inference as this provides uncertainty measures about the result. The application of Bayesian inference to identify Matérn kernel based microstructure generators was proposed in [8].

The idea is to identify Matérn covariance properties giving rise to surrogate microstructures having similar covariance and volume fraction as the original sample. The microstructures are characterized by the two point correlation function  $S_2$  that is further explained in [10]. Generally, this can be written as

$$S_2(\mathbf{x}_1, \mathbf{x}_2) = \langle \chi(\mathbf{x}_1, \omega) \chi(\mathbf{x}_2, \omega) \rangle_{\omega},$$

where  $S_2$  is approximated by the ensemble average (angular brackets) over multiple realizations. Assuming a random field is homogeneous, the  $S_2$  function does not depend on  $\mathbf{x}_1$ ,  $\mathbf{x}_2$  but on the vector between the points  $\mathbf{r} = \mathbf{x}_1 - \mathbf{x}_2$ . This leads to

$$S_2(\mathbf{r}) = \langle \chi(\mathbf{x}, \omega) \chi(\mathbf{x} + \mathbf{r}, \omega) \rangle_{\mathbf{x}, \omega},$$

where the ensemble average over all points  $\mathbf{x}$  in the spatial domain and all realizations  $\omega$  is computed. Following [10], limits of this homogeneous  $S_2$  function can be related to the volume fraction  $\phi$  through  $\phi = \lim_{|\mathbf{r}| \rightarrow 0} S_2(\mathbf{r})$ .

In order to identify the parameters  $\theta$  from this descriptor using Bayesian inference, the likelihood for the model parameters given some data needs to be derived.

From Bayes' rule it can be seen that

$$p(\theta|S_2^{\text{data}}) \propto p(\theta)p(S_2^{\text{data}}|\theta), \quad (5)$$

where  $p(\theta|S_2^{\text{data}})$  is the desired posterior probability,  $p(\theta)$  is the prior and  $p(S_2^{\text{data}}|\theta)$  is the likelihood of some specific measurements given  $\theta$ .

$$\begin{aligned} S_2^{\text{data}}(\mathbf{r}) &: \text{Covariance of Sample} \\ \mathbf{r} &: \text{Separation} \\ \theta &: \text{Model Parameters} \\ S_2(\theta, \mathbf{r}) &: \text{Model Covariance given } \theta \end{aligned}$$

This leads to the following model:

$$\begin{aligned} S_2^{\text{data}}(\mathbf{r}_i) &= S_2(\theta, \mathbf{r}_i) + \varepsilon \\ \varepsilon &\sim N(0, \sigma) \\ \varepsilon &\text{ independent of } \mathbf{r}_i \end{aligned}$$

Using this, the probability of each  $S_2^{\text{data}}(\mathbf{r}_i)$  originating from  $S_2(\mathbf{r}_i, \theta)$  given  $\mathbf{r}_i$  can be described by a normal distribution with

$$p_i(S_{2,i}^{\text{data}}|\mathbf{r}_i, \theta, \sigma) = \frac{1}{\sqrt{2\pi\sigma^2}} \exp\left(-\frac{(S_2^{\text{data}}(\mathbf{r}_i) - S_2(\theta, \mathbf{r}_i))^2}{2\sigma^2}\right).$$

Given  $n$  samples  $\underline{\mathbf{r}} = \{\mathbf{r}_i; i = 1..n\}$ , the likelihood can be rewritten as

$$\begin{aligned} p(S_2^{\text{data}}|\underline{\mathbf{r}}, \theta, \sigma) &= \prod_{i=1}^n \frac{1}{\sqrt{2\pi\sigma^2}} \exp\left(-\frac{(S_2^{\text{data}}(\mathbf{r}_i) - S_2(\theta, \mathbf{r}_i))^2}{2\sigma^2}\right) \\ &= \frac{1}{\sqrt{2\pi\sigma^2}^n} \exp\left(-\frac{\sum_{i=1}^n (S_2^{\text{data}}(\mathbf{r}_i) - S_2(\theta, \mathbf{r}_i))^2}{2\sigma^2}\right). \end{aligned}$$

Thus, the log likelihood can be written as

$$L(\theta, \sigma) = -\frac{n}{2} \log 2\pi - n \log \sigma - \frac{1}{2\sigma^2} \sum_{i=1}^n (S_2^{\text{data}}(\mathbf{r}_i) - S_2(\theta, \mathbf{r}_i))^2. \quad (6)$$

To get the posterior likelihood, 6 needs to be related to an appropriately chosen prior distribution using 5. For the log posterior, this leads to

$$P(\theta, \sigma) = L(\theta, \sigma) + \log(\text{Prior}) - \text{constant}, \quad (7)$$

where the constant is related to the *evidence* from Bayes' rule. With this log posterior likelihood, samples from the posterior distribution 5 can be obtained using Markov Chain Monte Carlo as implemented in the python tool *pymc* [1]. Using these samples, a posterior analysis can be conducted giving rise to confidence intervals on the parameters and maximum a posteriori (MAP) estimators.

### 3 Results

To demonstrate the viability of this approach, a sample  $\chi^{\text{data}}$  is generated from a Matérn random field using the approach laid out in 2.1. The parameters (ie. ground truth parameters) are then identified using the computational procedure in 2.2.

Based on the material image, the posterior distribution is sampled using the derived likelihood 7 and a uniform prior distribution within the accepted bounds of correlation length (0, 1.) and volume fraction (0, 1.). The standard deviation of the noise  $\sigma$  is also inferred and the prior is modeled by an exponential distribution with  $\lambda = 1$ , which is a common approach as the standard deviation must be positive.

The sampling is conducted using pymc's slice sampler with 50000 samples. The estimation of the surrogate material properties give an 97% interval for the volume fraction of the material to be between 0.19 and 0.20 with a maximum a posteriori value  $\tau_{\text{MAP}} = 0.19$ . With the ground truth being 0.2, this is thus accurately recovered. The correlation length has a posterior confidence interval between  $[0.0043, 0.0055]$  with  $l_{\text{MAP}} = 0.0049$  with the ground truth being 0.005. Thus, for both cases, the parameters of the covariance kernel (3) and the level set cutoff (2) are accurately recovered.

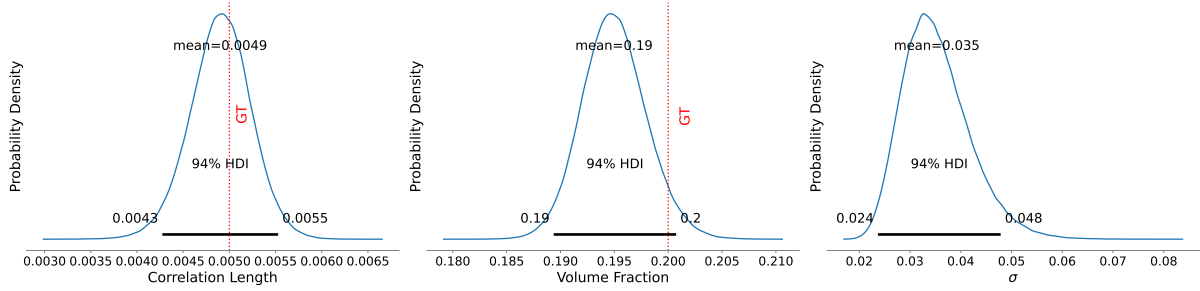


Figure 3: Posterior Distribution of Correlation Length, Volume Fraction and  $\sigma$  Reconstruction based on given  $\chi$  image

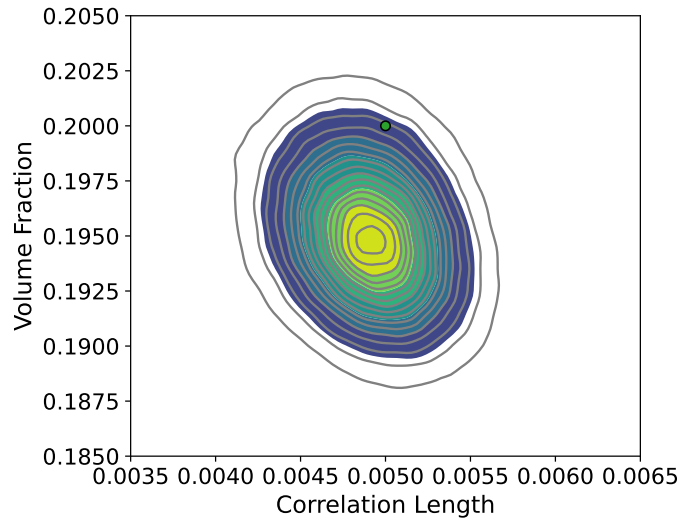
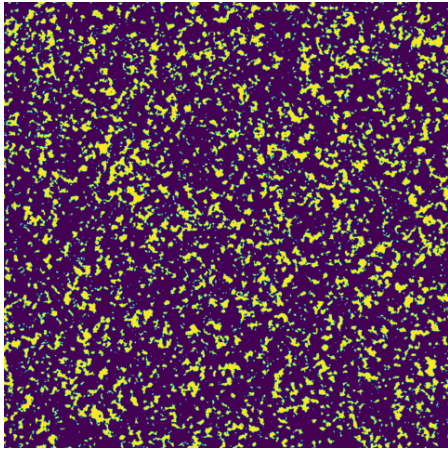
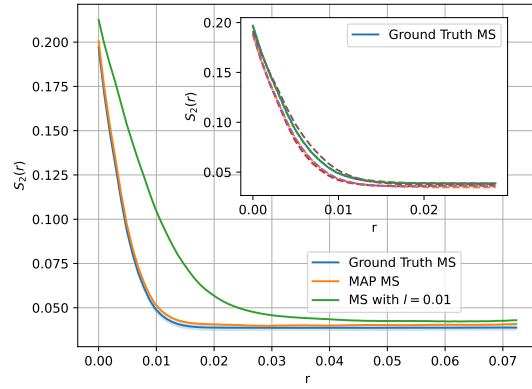


Figure 4: Pair Plot of Posterior Distribution of Volume Fraction and Correlation Length

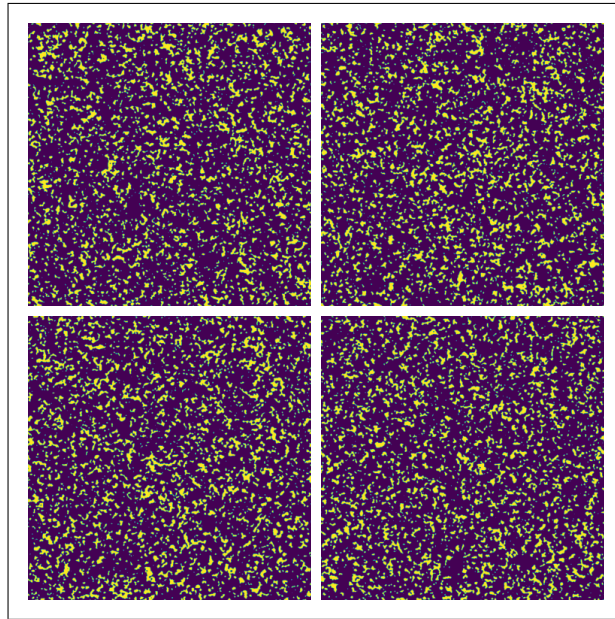
The difference between the ground truth specimen, which is reconstructed and specimens generated from the posterior distribution in 3 can be seen in figure 5. The ground truth microstructure to be identified can be seen in figure 5a. In figure 5b differences in the  $S_2$  correlation function between the ground truth and the reconstructed parameters are shown. The  $S_2$  correlation functions shown in the detail are sampled from the identified posterior distribution which is used in figure 5c as well.



(a) Ground truth microstructure to be identified, Resolution of 1024x1024 points



(b) Difference in  $S_2$  correlation functions of ground truth microstructures,  $S_2$  correlation function and different  $S_2$  correlation functions for samples from posterior 3



(c) Samples from posterior distribution in 3, (Resolution of 1024x1024 points)

Figure 5: Reconstruction results after Bayesian Inference compared to input microstructure

## 4 Conclusion and Perspectives

The identification of microstructures governed by Gaussian random fields has been shown to be feasible. The covariance and level set parameters based on which the ground truth sample was generated has been recovered. Furthermore, the use of metamodelling techniques paths the way for future computationally more expensive problems. Due to the application of methods of statistical inference in the reconstruction of microstructural parameters, the obtained results chain in well to the application of uncertainty problems.

The potential extensions can be classified into two parts. The first part includes the application onto the direct identification and generation of microstructures. Here, experimentally obtained EBSD,  $\mu$ CT or SEM data can be used in a first step to show the feasibility of the approach and the functioning of the toolbox. Furthermore, the application to external SEM data can be studied, for example the data given in [6]. A sample from this microstructure can be seen in figure 1 and the similarity to the samples generated in figure 2 can be studied. In [8], the random field microstructure generator was extended to include an underlying topological support, meaning it can capture more complex microstructures. Here, first an ideal microstructure without noise is generated which is distorted based on its level set description.



Depending on the specimen studied, this extension should be included. This leads to the capability of studying more complex structures whilst accounting for deviations from ideal geometries. Depending on the problem studied, additional geometric microstructure descriptors can be included. They can be augmented through the use of mechanical descriptors such as effective mechanical behaviour.

Additionally, the resulting identified microstructure generator should be applied onto more complex failure assessment types. Here, the sampling methods introduced can be used for *rare event* problems. This includes problems of high cycle fatigue, where each individual failure has a low likelihood, but the results can be catastrophic and the structure is studied over a long period of time. A potential failure mechanism to be studied in this field is the Dang-Van fatigue criterion, which fits well into the periodic microstructure setting [5, 11, 4]. The current solution of the elasticity problem can directly be extended to crystal plasticity, thus being applicable for various failure models and being capable of accurately describing different phenomena of metallic structures. Some initial steps in this application were conducted in [8, 9].

## References

- [1] O. Abril-Pla et al. *PyMC: a modern, and comprehensive probabilistic programming framework in Python*. en. In: PeerJ Computer Science 9 (Sept. 2023), e1516.
- [2] S. Bargmann et al. *Generation of 3D representative volume elements for heterogeneous materials: A review*. en. In: Progress in Materials Science 96 (July 2018), pp. 322–384.
- [3] D. G. Brandon and W. D. Kaplan. *Microstructural characterization of materials*. eng. 2. ed., repr. Quantitative software engineering series. Chichester: Wiley, 2010.
- [4] E. Charkaluk et al. *Revisiting the Dang Van criterion*. en. In: Procedia Engineering 1.1 (July 2009), pp. 143–146.
- [5] K. Dang Van and I. V. Papadopoulos. *High-cycle metal fatigue: from theory to applications*. eng. CISM Courses and lectures 392. Wien New York: Springer, 1999.
- [6] C. Griesbach et al. *Microstructural heterogeneity of the buffer layer of TRISO nuclear fuel particles*. en. In: Journal of Nuclear Materials 574 (Feb. 2023), p. 154219.
- [7] C. Griesbach et al. *Microstructural heterogeneity of the buffer layer of TRISO nuclear fuel particles: Meshes of pores*. Creative Commons Attribution 4.0 International. 2022.
- [8] U. Khristenko et al. *A Statistical Framework for Generating Microstructures of Two-Phase Random Materials: Application to Fatigue Analysis*. en. In: Multiscale Modeling & Simulation 18.1 (Jan. 2020), pp. 21–43.
- [9] U. Khristenko et al. *Statistically equivalent surrogate material models: Impact of random imperfections on the elasto-plastic response*. en. In: Computer Methods in Applied Mechanics and Engineering 402 (Dec. 2022), p. 115278.
- [10] S. Torquato. *Random Heterogeneous Materials*. Ed. by S. S. Antman et al. **16**. Interdisciplinary Applied Mathematics. New York, NY: Springer New York, 2002.
- [11] K. Van and M. Maitournam. *On some recent trends in modelling of contact fatigue and wear in rail*. en. In: Wear 253.1-2 (July 2002), pp. 219–227.